International Journal of Energy and Water Resources
https://doi.org/10.1007/s42108-025-00355-x

ORIGINAL ARTICLE

# Nanoparticle-assisted ternary fuel blends: an investigation of diesel engine performance, combustion and emission profiles

**B. D. Potnuru**[1] · **N. V. N. Indra Kiran**[2] · **J. Sagari**[3]

Received: 4 October 2024 / Accepted: 4 March 2025

## Abstract

The main objective of this study is to evaluate the operating parameters of a diesel engine running on a ternary fuel mixture in combination with titanium oxide nanoparticles. Two separate feedstocks namely *Ricinus communis* and *Cassia fistula* were combined to produce the hybrid biodiesel. Three different alcohols-iso-butanol, iso-propanol, and n-butanol each accounting for 5% of the total volume were also added to the biodiesel blend. To increase stability, an additional 75 ppm titanium oxide nanoparticles were accompanied to the ternary fuel. The ternary fuel mixture improved the brake thermal efficiency and slightly reduced the brake specific fuel consumption. Combustion characteristics such as the net heat release rate and cylinder pressure were likewise amended. Emissions of carbon monoxide, unburned hydrocarbons, and smoke have also been reduced. However, emissions of nitrogen oxides increased. By introducing nanoparticles into the ternary fuel mixture, both performance and combustion behaviour were improved, while emissions, especially nitrogen oxides, were significantly reduced. The biodiesel blend with 5% n-butanol and 75 ppm nanoparticles addition achieved the best results, and the specific brake fuel consumption was 0.173 kg/kWh, accompanied by a thermal braking efficiency of 26.91%. The cylinder pressure reached a maximum value of 68.12 bar and the net heat release rate reached 70.14 J/°CA. Emissions of 0.051% for carbon monoxide, 31 ppm for unburned hydrocarbons, 1245 ppm for nitrogen oxides and 32.63% for smoke opacity were measured.

**Keywords** Biodiesel · Alcohol · Nanoparticles · Brake thermal efficiency · Cylinder pressure · Carbon dioxide

## Abbreviations

| | |
|---|---|
| SDS | Sodium dodecyl sulfate |
| BTE | Brake thermal efficiency (%) |
| BSFC | Brake specific fuel consumption (kg/kWh) |
| CP | Cylinder pressure (bar) |
| NHRR | Net heat release rate (J/°CA) |
| CO | Carbon monoxide (%) |
| UHC | Unburnt hydrocarbons (ppm) |
| $NO_x$ | Oxides of nitrogen (ppm) |
| $TiO_2$ | Titanium oxide |
| NPs | Nanoparticles |
| GO | Graphene oxide |
| GNPs | Graphene nanoparticles |
| MWCNTs/CNTs | Multi-walled carbon nanotubes/Carbon nanotubes |
| DMC | Dimethyl carbonate |
| DEE | Diethyl ether |
| EGM | Ethylene glycol monoacetate |
| TGME | Tri-ethylene glycol monomethyl |
| NaOH | Sodium hydroxide |
| XRD | X-ray diffraction |
| SEM | Scanning electron microscopy |
| B20 | 20% Hybrid biodiesel + 80% diesel |
| $Fe_2O_3$ | Ferric oxide |

## Introduction

Two major obstacles facing the global research community are the rapid depletion of fossil fuel supplies and the complexities arising from pollution and global warming. A major sector that is largely dependent on the use of fuels

✉ J. Sagari
sagari.jaikumar1@gmail.com

B. D. Potnuru
baladivyapotnuru@gmail.com

[1] AU Trans-Disciplinary Research Hub (A.U.TDR-HUB), Andhra University, Visakhapatnam, India

[2] Department of Mechanical Engineering, Anil Neerukonda Institute of Technology, Visakhapatnam, India

[3] School of Marine Engineering and Technology, Indian Maritime University, Kolkata, India

and causes negative emissions is the transportation sector (El-Seesy et al., 2020; Jaikumar et al., 2021). Because of their great thermal efficiency, durability, and strong construction, compression ignition engines are regularly used in industrial and commercial vehicles, marine propulsion systems, and power generators. But fast technical developments and economic expansion have presented the energy industry more difficulties lately. Given the scale of these problems and the possibility of an energy crisis, researchers and scientists have focused on the development of renewable energy sources that can either partially or completely swap traditional petroleum-based fuels (El-Seesy et al., 2021; Garugubilli et al., 2024). Biodiesel is appropriate as a supernumerary for diesel owing to its advantageous physico-chemical properties and its increased oxygen content (Mahlia et al., 2020; Saravanan et al., 2020a, 2020b). Commercialization of biodiesel in the transportation sector faces challenges such as poor atomization, higher viscosity, higher oxides of nitrogen ($NO_x$) emissions, low brake specific fuel consumption (BSFC) and problems with cold flow and cold start performance. These drawbacks can be addressed through innovative approaches, including the incorporation of oxygenated alcohols and nanoparticles as additives (Kari et al., 2024; Sayyed et al., 2023). Nanoparticles and alcohols are of great interest as fuel additives for compression ignition engines. Conversely, nanoparticles are confirmed to be an excellent approach to reduce $NO_x$ and carbon emissions while improving engine performance, including brake thermal efficiency (BTE) and BSFC (Illipilla et al., 2023; Reddy et al., 2023; Saravanan et al., 2020a, 2020b). Srikanth et al. (2021) considered the impact of biodiesel and ethanol on diesel engine performance. Their findings revealed that adding ethanol in biodiesel blend enhanced BTE, shortened BSFC, and significantly lowered emissions. Senthil and Rajan (2022) experimented with a mixture of rubbur seed oil biodiesel and Dimethyl carbonate (DMC) alcohol in different dosages. They originate that overall performance was upgraded and $NO_x$ emissions and soot opacity were significantly lower than with conventional diesel. Rangabashiam et al. (2024) explored neem biodiesel blended with DMC and pentanol. They concluded that BTE was improved and BSFC was reduced when DMC and pentanol were added to biodiesel, while carbon monoxide (CO) and unburnt hydro carbons (UHC) were greatly reduced. Nutakki et al. (2022) examined the effects of ferric oxide ($Fe_2O_3$) nanoparticles on a ternary fuel mixture. Their work demonstrated a reduction in $NO_x$, CO, and UHC emissions, while the performance parameters have achieved a positive result. El-Seesy et al. (2019) examined the effects of graphene oxide (GO), graphene nanoparticles (GNPs), and multi walled carbon nanotubes (MWCNTs) in alcohol added biodiesel and diesel. Their study exposed that the cylinder pressure amplified because of the dispersion of nanoparticles in the ternary fuel mixture, while the emission of $NO_x$, UHC, and CO was momentously reduced. Parida et al. (2024) considered a Karanja oil biodiesel blend with $TiO_2$ nanoparticles. They found that BTE was reduced by 1.72% and BSFC by 3.57%. Zhao et al. (2022) conducted a thorough examination of the impacts of higher alcohols, when combined with diesel fuel, with the aim of assessing the emissions and combustion characteristics. The findings indicate that the combustion parameters exhibited enhancement with the utilisation of larger alcohol blends; however, this was accompanied by an increase in the emission parameter, specifically $NO_x$. Liang et al. (2021) used n-pentanol and biodiesel in their exploration. They reported that an increase in cylinder pressure and a simultaneous reduction in CO emissions could be observed. Besides, the addition of n-pentanol to biodiesel together with exhaust gas recirculation (EGR) led to a reduction in $NO_x$ emissions. Killol et al. (2019) looked at the n-butanol and diethyl in biodiesel. Their study showed a remarkable reduction in CO emissions with a simultaneous increase in performance parameters. Chaurasiya et al. (2019) explored the influence of blending alcohols into biodiesel-diesel combination and found a significant improvement in net heat release (NHR) and BSFC. The results show that the enrichment of alcohols reduced emissions. Saxena et al. (2019) investigated the use of $TiO_2$ in a diesel engine powered by *Acacia Concinna* biodiesel. Their findings showed a decrease in BSFC, UHC, and smoke, along with an improvement in BTE. However, $NO_x$ exhibited only a slight increase.

In the existing literature, there is no study on the synergistic influence of alcohol and nanoparticles in biodiesel blends. Although previous research has investigated these compounds individually, their combined effect has not been studied. This study aims to integrate both alcohol and nanoparticles in hybrid biodiesel and evaluate their effects through experimental research. The use of hybrid biodiesel with these additives represents a new approach in this research.

The objectives of the present work are:

- Investigate the effects of hybrid biodiesel blended with higher alcohols (isobutanol, isopropanol, and n-butanol) on the performance, combustion, and emissions characteristics of diesel engines.
- Investigate the effect of $TiO_2$ nanoparticles in a ternary fuel mixture to estimate the functional characteristics of diesel engines under different load conditions.

The experiments were conducted between 15th April 2022 and 25th February 2023 in the Department of Mechanical Engineering at GITAM (Deemed to be University), Visakhapatnam, HPCL Visakhapatnam, and Lords Institute of Engineering and Technology, Hyderabad.

## Materials and methods

### Transesterification process

The oils from two different sources were extracted, purified, hybridised before transesterification the process. First, 600 mL of the hybrid oil was heated to 50 °C by means of a magnetic stirrer. Then a combination of sodium hydroxide (NaOH) and methanol was added stepwise to the heated oil. The mixture was transesterified at 60 °C for 90 min with constant stirring at 900 rpm. This process was carried out for each test series to obtain different biodiesel samples. The reaction mixture was then relocated to a conical conduit and left undisturbed for a full day to facilitate sedimentation of the glycerol by-product at the bottom. The top layer, which consisted of biodiesel, was carefully extracted and rinsed five to six times with hot water at 70 °C to remove any residue. A final heating phase at 100 °C removed the remaining moisture. The hybrid biodiesel produced using this technique had a yield of 96.4%. Figure 1 shows a schematic representation of the entire biodiesel production process.

### Characterization of nanoparticles

The X-ray diffraction (XRD) and scanning electron microscopy (SEM) patterns of $TiO_2$ nanoparticles are shown in Fig. 2a, b. The specifications of the XRD and SEM analyses are shown in Tables 1 and 2, respectively. The XRD

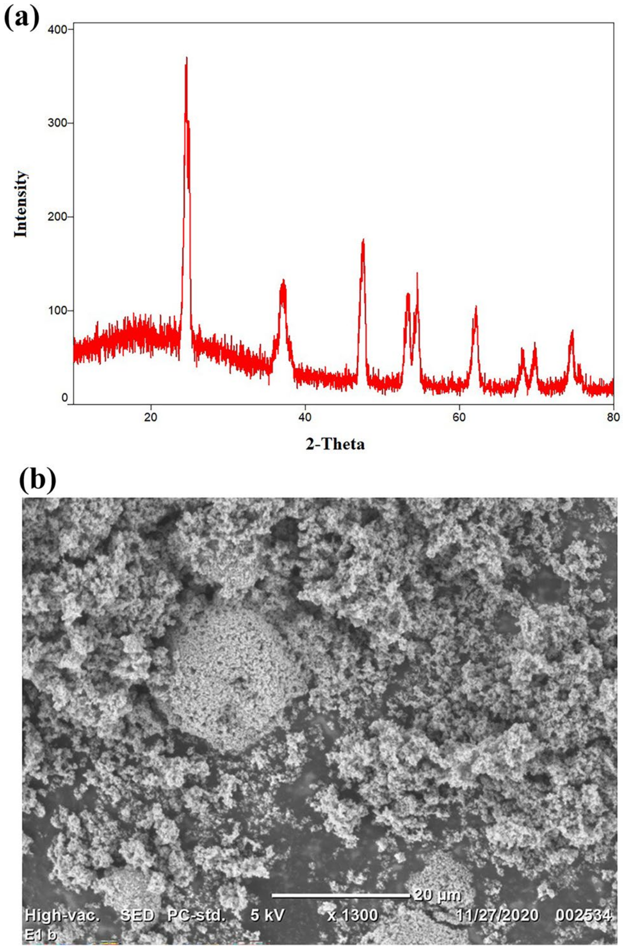

**Fig. 2** **a** XRD of $TiO_2$ nanoparticles. **b** SEM image of $TiO_2$ nanoparticles

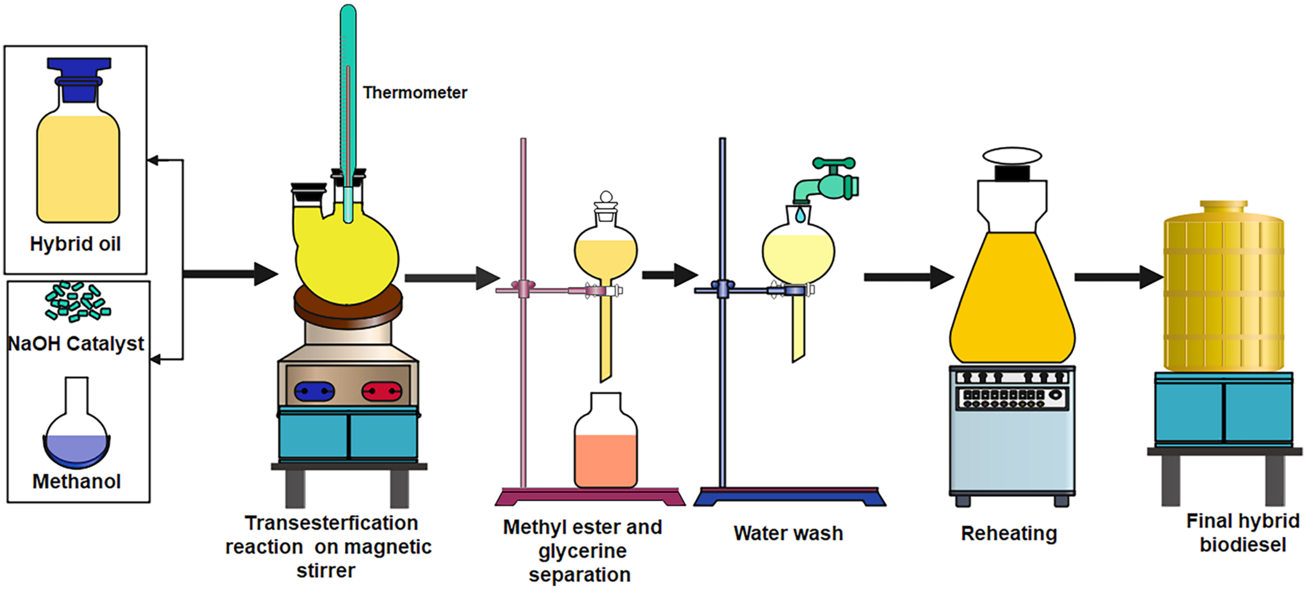

**Fig. 1** Biodiesel preparation

**Table 1** Specifications of XRD

| Parameter | Description |
|---|---|
| Make | Bruker (Germany) |
| Model | Bruker D8 advance |
| Cu K radiation (Å) | 1.5406 |
| Scanning rate | 0.01° |
| Voltage (kV) | 40 |
| Angle 2θ | Ranging from 10° to 80° |

form displays a vibrant, rigid and distinct peak at an angle of 2θ = 69.78°, indicating a clear crystalline structure with particle size of about 12 nm. Besides, the SEM image shows the surface morphology of the nanoparticles and highlights the presence of lighter areas, indicating the crystalline structure.

### Ternary nanofuel preparation

Three blends are prepared by combining iso-butanol, isopropanol, and n-butanol at a concentration of 5% by volume with a combination of 20% hybrid biodiesel (i.e. *Cassia fistula* and *Ricinus communis*) and 80% diesel fuel. The ultrasonic sonication method is then used to homogeneously diffuse $TiO_2$ nanoparticles (75 ppm) in ternary fuel mixture. In addition, the $TiO_2$ nanoparticles at a concentration of 75 mg/L and a corresponding amount of SDS were collected in a beaker and the hexane was added to it. The samples were sonicated in an ultrasonic bath at a continuous temperature of 35 °C for forty minutes before drying. After drying, the ternary nanofuel was combined with $TiO_2$ nanoparticles using an ultrasonic probe. The procedure was carried out for 15 min with each individual sample.

### Stability analysis

The photo spectrometer was used to evaluate the stability in terms of transmittance. Table 3 lists the specific parameters of the spectrophotometer. The variation of transmittance (stability) is shown in Fig. 3. After a seven-day preparation period, the nanofuel sample was analysed. Of the three samples analysed, the n-butanol-based nanofuel together with the SDS surfactant exhibited the lowest stability. The transmittance of B20 in combination with 5% isobutanol with 75 ppm nanoparticles, 5% isopropanol with 75 ppm nanoparticles and 5% n-butanol with 75 ppm nanoparticles is 94.71%, 91.54% and 86.50%, respectively. Finally, the properties of the fuel samples were evaluated based on ASTM standards (see Table 4).

**Table 2** Specification of the SEM

| Parameter | Description |
|---|---|
| Make | USA |
| Model | ALPHA-II |
| Source | IR source, air cooled, 12 V, 20 W |
| Beam splitter | Zinc resolution (ZnSe) |
| Detector | High resolution DTGS detector |
| Range ($cm^{-1}$) | 4000–500 |

**Table 3** Specifications of the photo spectrometer

| Parameter | Description |
|---|---|
| Start (nm) | 1100 |
| Stop (nm) | 200 |
| X mode | Nanometers |
| Absorbance/transmittance UV–vis scan rate (nm/min) | 2400 |
| UV–vis data interval (nm) | 5 |
| UV–vis ave. time (s) | 0.0125 |
| Beam mode | Dual beam |

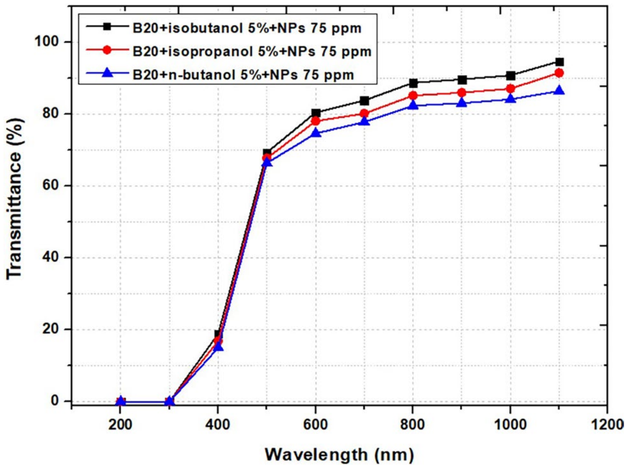

**Fig. 3** Transmittance of nanofuel

## Experimental test rig and procedure

In this investigation, the compression ignition engine operating characteristics assessed on a single cylinder diesel engine. Figure 4 displays a graphical representation of the test configuration while Table 5 contains the practical specifications. The fuel tank was connected to a fuel flow sensor. The performance was evaluated based on the duration of fuel degradation. It was also possible to calculate the combustion parameters with the Engine soft program. The emissions were measured with a gas analyser and smoke meter. The connection between the combustion sensor and the crank

**Table 4** Properties of fuel samples

| Property | Kinematic viscosity, cSt (ASTM D445) | Heating value, kJ/kg (ASTM D4809) | Cetane index (ASTM D4809) | Density, kg/m$^3$ (ASTM D4809) | Flash Point, °C, (ASTM D4809) |
|---|---|---|---|---|---|
| ASTM range | 2.3–6 | 42,000 | 47 (min.) | 860–900 | 132 (min.) |
| Diesel | 3.72 | 44,000 | 52 | 830 | 55 |
| B100 | 4.53 | 39,862 | 58 | 887 | 162 |
| B20 | 3.62 | 40,798 | 57 | 871 | 109 |
| B20 + isobutanol 5% | 3.71 | 39,865 | 56 | 874 | 106 |
| B20 + isopropanol 5% | 3.68 | 39,731 | 56 | 877 | 108 |
| B20 + n-butanol 5% | 3.65 | 39,667 | 56 | 879 | 107 |
| B20 + isobutanol 5% + NPs75 ppm | 3.76 | 40,823 | 59 | 876 | 111 |
| B20 + isopropanol 5% + NPs 75 ppm | 3.72 | 40,876 | 59 | 879 | 114 |
| B20 + n-butanol 5% + NPs 75 ppm | 3.69 | 40,823 | 60 | 881 | 116 |

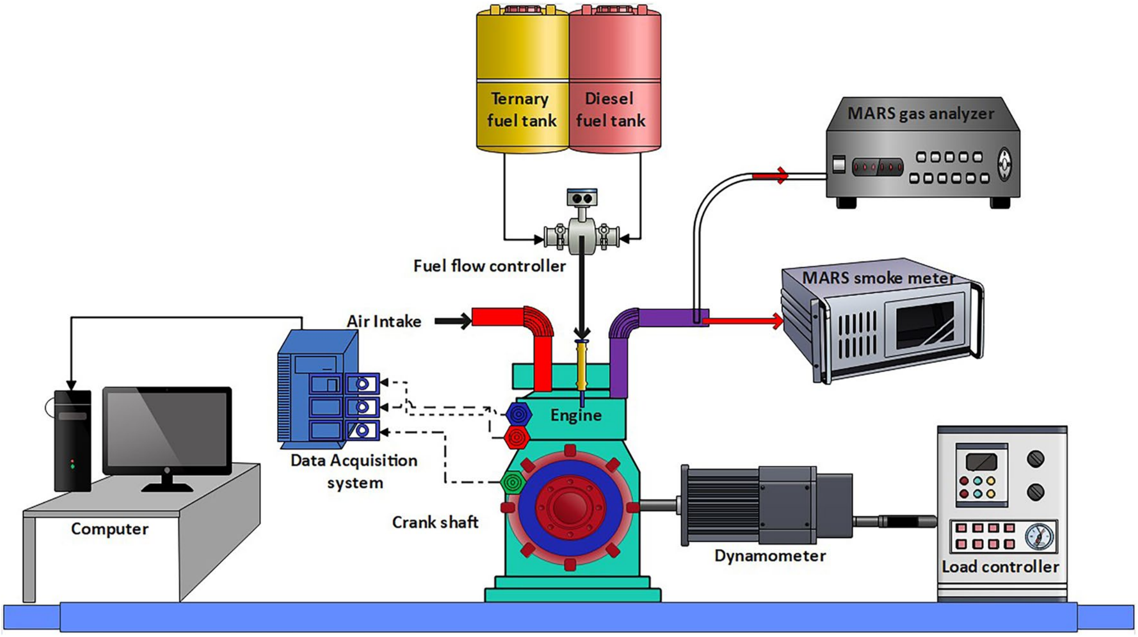

**Fig. 4** Graphical illustration of experimental test rig

**Table 5** Technical data of diesel engine test rig

| Constraint | Details |
|---|---|
| BP (kW) and make | 3.5 and Kirloskar |
| Speed (RPM) | 1500 |
| Engine load (kgf) | 3, 6, 9, and 12 |
| Injection pressure (bar) | 225 |
| Number of cylinders | 1 |
| Compression ratio | 18 |
| Bore (mm)/stroke (mm) | 87.5/110 |
| Fuel flow sensor | Make Yokogawa Japan, DP transmitter, range 0–500 mmWC |

angle sensor to the personal computer was detected via a DAQ.

The current investigation commenced with a 25-min preparation stage of the engine with diesel fuel from the main tank and consisted of several phases of experimental tests. The fuel supply is checked to guarantee that the engine is receiving the essential fuel supply for the required operating level. The engine speed is regulated to 1500 rpm while maintaining a constant compression ratio of 18. The data obtained from the various devices is examined in detail under controlled conditions. The procedure was repeated at 25, 50, 75, and 100% loading for all the fuels prepared. Each test was performed three times to ensure the consistency of the data. These results were then compared with those of pure diesel fuel.

## Uncertainty analysis

Uncertainty analysis affords a comprehensive valuation of experimental reproducibility and deals with the deviations in measurements. It includes the evaluation of errors resulting from experimental methods, observed precision, calibration and the use of equipment. Equations (1) and (2) give the total and parameter-specific uncertainties

$$R_L = \sqrt{\left\{ \left(\frac{\delta L}{\delta x} R_1\right)^2 + \left(\frac{\delta L}{\delta x} R_2\right)^2 + \left(\frac{\delta L}{\delta x} R_3\right)^2 + \cdots \left(\frac{\delta L}{\delta x} R_N\right)^2 \right\}} \tag{1}$$

$R_L$ stands for the aggregated or total uncertainty, L denotes the function of uncertainty and $R_1$ to $R_N$ stand for the uncertainties of the specific adjustables. Table 6 shows the specific instrumental uncertainty.

The total uncertainty is calculated using the following equation:

$$\begin{aligned} \textit{Uncertainty in total} &= \sqrt{\left\{ \begin{array}{c} (\Delta BTE)^2 + (\Delta BSFC)^2 + (\Delta CP)^2 \\ +(\Delta NHRR)^2 \\ +(\Delta \mathrm{CO})^2 + (\Delta UHC)^2 \\ +(\Delta \mathrm{NOx})^2 + (\Delta\, smoke)^2 \end{array} \right\}} \\ \textit{Uncertainty in total} &= \sqrt{\left\{ \begin{array}{c} (1.9)^2 + (1.8)^2 + (0.6)^2 \\ +(0.8)^2 \\ +(1.3)^2 + (1.6)^2 \\ +(0.9)^2 + (1.1)^2 \end{array} \right\}} \end{aligned} \tag{2}$$

The total uncertainty is ± 3.75%.

**Table 6** Instrumental accuracy and uncertainty

| Measurement parameter | Accuracy | Uncertainty (%) |
|---|---|---|
| Load (kg) | ± 0.2 kg | ± 0.1 |
| Speed (rpm) | ± 30 rpm | ± 0.1 |
| Arm length (m) | ± 0.001 m | ± 0.01 |
| Fuel burette measurement (cc) | ± 1 cc | ± 0.01 |
| Stop watch (s) | ± 0.2 s | ± 0.02 |
| Piezo sensor (bar) | ± 0.1 bar | ± 0.1 |
| Crank angle sensor (°) | ± 1° | ± 0.1 |
| CO (%) | ± 0.1% | ± 1.3 |
| $NO_x$ (ppm) | ± 20 ppm | ± 1.6 |
| UHC (ppm) | ± 10 ppm | ± 0.9 |
| Smoke opacity (%) | ± 1% | ± 1.1 |

## Results and discussion

### Performance characteristics

#### BTE

Figure 5 illustrates the variation in the BTE in terms of load. It can be observed that the ternary fuel blends have a better BTE value than diesel and B20 alone. The improved combustion and the considerable improvement in BTE were the result of the abundant presence of oxygen molecules in isobutanol, isopropanol and n-butanol (El-Seesy et al., 2020; Sayyed et al., 2023; Killol et al., 2019; Liang et al., 2021). This is due to the faster flame speed (Liang et al., 2021; Potnuru et al., 2025). Besides, the $TiO_2$ nanoparticles accumulation to the alcohol compositions resulted in better BTE. The main reason for this improvement seems to be the catalytic ability of the nanoparticles, which enables the micro-explosion. The enlarged contact area of the $TiO_2$ nanoparticles, in addition to their high reactivity and energy storage capacity, is a key factor contributing to the improvement in BTE (Garugubilli et al., 2024; Illipilla et al., 2023; Jaikumar et al., 2021; Saxena et al., 2019). At higher loads, the BTE was greater, as higher cylinder pressures and temperatures reduce heat losses to the surrounding components and the coolant. With these heat losses, the energy is converted into productive energy. The BTE values at full load varied from 24.03 to 26.91% for the different fuel blends. In particular, B20 showed the lowest BTE at 24.03%, while the highest value of 26.91% was obtained for the B20 blend with 5% n-butanol and 75 ppm nanoparticles. The combination of B20, n-butanol (5%) and nanoparticles (75 ppm) showed the best performance among the evaluated fuels.

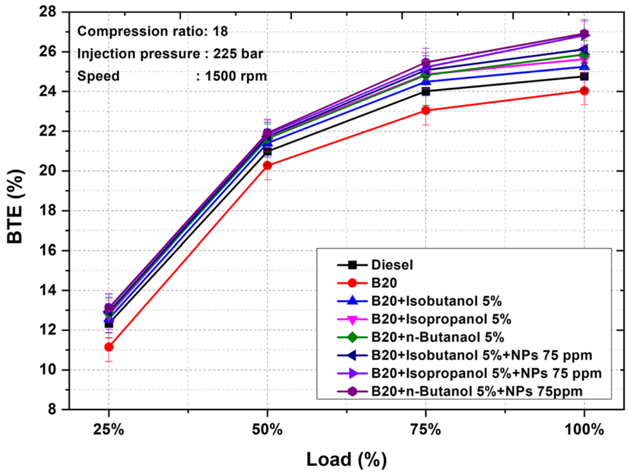

**Fig. 5** BTE versus load

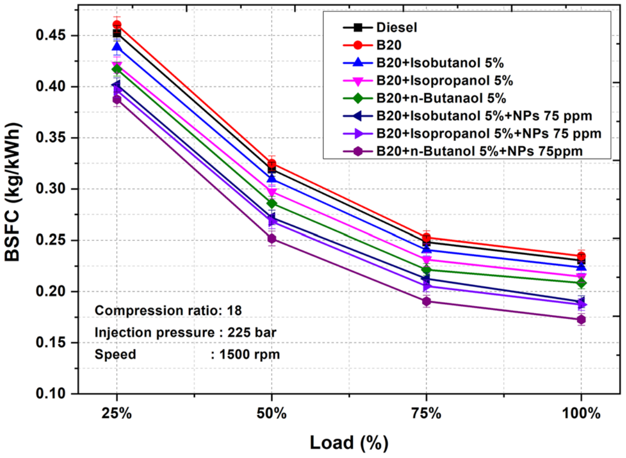

**Fig. 6** BSFC versus load

### BSFC

The change of BSFC for different ternary fuel blends and fuel samples enriched with nanoparticles are shown in Fig. 6. The BSFC of B20 shows an increase than regular diesel. Nevertheless, the alcohols addition to B20 directed to a drop in BSFC than diesel. Since the oxygenated ternary fuel blends had a lower BSFC due to their lower kinematic viscosity, resulting in a better air–fuel mixture and better atomization (Mobasheri et al., 2023; Potnuru et al., 2025; Preuß et al., 2018; Srikanth et al., 2021). These fuels enable a more complete combustion process and have a higher flame propagation rate, which improves the conversion of chemical energy into mechanical energy (El-Sheekh et al., 2022; Zuo et al., 2022). Also, an additional decrease in BSFC was perceived when $TiO_2$ nanoparticles were dispersed into ternary fuel mixtures with different alcohols. This decrease can be attributed to the high cetane number of $TiO_2$ nanoparticles, the low physical retardation and the large contact area. Improved spray diffusion and a higher evaporation rate reduce the BSFC (Garugubilli et al., 2024; Illipilla et al., 2023; Jaikumar et al., 2021; Kunchi et al., 2024; Saxena et al., 2019). Finally, lowering the BSFC at higher loads and cylinder pressures enabled better combustion of the fuel–air combination. At full load, B20 had the highest BSFC of 0.235 kg/kWh, while the lowest BSFC was 0.173 kg/kWh for the combination of B20, 5% n-butanol and 75 ppm nanoparticles.

## Combustion characteristics

### CP

Figure 7 displays CP versus crank angle for ternary fuel mixtures with dispersed $TiO_2$ nanoparticles. This is due to the fact that the biodiesel can have an oxygenated behaviour and more cetane number. This resulted in a stronger atomization of the fuel and better combustion (Chaurasiya et al., 2019; Jaikumar et al., 2021; Kunchi et al., 2024). Furthermore, the CP was augmented by the introduction of alcohol additives in B20. The increased latent heat of vaporisation of alcohols increases the vaporisation of fuel. Cooling the air–fuel mixture as it enters the cylinder improves its density, which leads to better combustion and thus to an increase in CP. The presence of nanoparticles in alcohol mixtures significantly amended CP dispersion (Nutakki et al., 2022; Anantha and Mohanty 2024; Killol et al., 2019). This is primarily due to the increased surface-to-volume ratio and the improved thermal conductivity of the $TiO_2$ nanoparticles. In addition, the oxygenated imprint of the $TiO_2$ nanoparticles and alcohol in B20 increased the CP, which is due to a stronger homogenization of the fuel (Jaikumar et al., 2021; Kari et al., 2024; Illipilla et al., 2023; Reddy et al., 2023). At a loading concentration of 100%, diesel alone had the lowest CP at 55.57 bar, while B20 in combination with 5% n-butanol and 75 ppm nanoparticles achieved the highest CP at 68.12 bar.

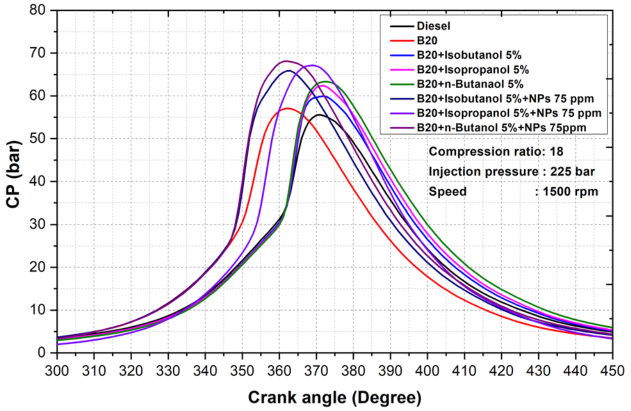

**Fig. 7** CP versus crank angle

### NHRR

Figure 8 illustrates the NHRR compared to the crank angle. The net NHRR of B20 is a little advanced than that of diesel attributable to the increased fuel uptake caused by the ignition delay, and the high oxygen content contributes to this result (Jaikumar et al., 2021; Saravanan et al., 2020a, 2020b; Kari et al., 2024; Potnuru et al., 2025). Additionally, the NHRR of the B20 blend, which contains the alcohols isobutanol, isopropanol and n-butanol, exceeds that of pure diesel fuel. The reason for this is that alcohol has a higher latent heat of vaporisation and a greater amount of oxygen. Despite the lower calorific value and longer ignition delay, alcohols ignite quickly, resulting in a higher NHRR (El-Seesy et al.,

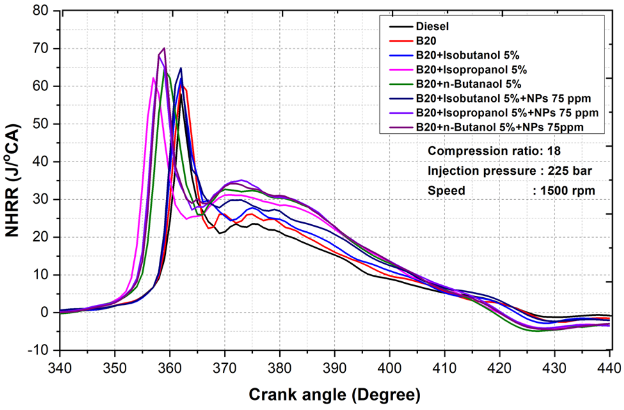

**Fig. 8** NHRR versus crank angle

2020; Garugubilli et al., 2024; Srikanth et al., 2021). An increase in NHRR was noticed when $TiO_2$ nanoparticles diffused into isobutanol, isopropanol and n-butanol. This was a result of the enhanced heat transfer from the $TiO_2$ nanoparticles to B20 as well as the catalytic activity (Illipilla et al., 2023; Kunchi et al., 2024; Reddy et al., 2023). The evaporation of the fuel and the heat loss via the cylinder walls both contributed to a reduction in heat dissipation (Kunchi et al., 2024). At maximum exposure, diesel had the lowest NHRR at 57.96 J/°CA, while the combination of B20, 5% n-butanol and 75 ppm nanoparticles achieved the highest NHRR at 70.14 J/°CA.

## Emission characteristics

### CO

Figure 9 illustrates the distinction in CO with load and clearly shows that B20 and ternary fuel combinations deliver pointedly inferior CO values. The reason for this is that biodiesel contains a higher proportion of oxygen and has a higher cetane number. The presence of alcohol in the biodiesel makes it easier for the engine to operate with a higher concentration of air in the fuel mixture and increases the amount of oxygen available for combustion. To minimize the formation of CO, the amount of fuel in the mixture must be reduced to such an extent that there is enough oxygen to completely convert the carbon in the fuel into $CO_2$ instead of CO (Potnuru et al., 2025; Sayyed et al., 2023; Nutakki et al., 2022; Zhao et al., 2022; Liang et al., 2021). Furthermore, a decrease in CO content was observed when $TiO_2$ nanoparticles were uniformly dispersed in ternary fuel mixtures based on isobutanol, isopropanol and n-butanol. The addition of $TiO_2$ nanoparticles reduces the ignition delay by accelerating the combustion of the fuel in the cylinder through rapid combustion reactions, and of course the conversion of $CO_2$ to CO is also accelerated (Jaikumar et al., 2021; Kari et al., 2024; Illipilla et al., 2023; Reddy et al., 2023; Kunchi et al., 2024). At higher loads, CO augmented as a result of the increased power requirement, which results in a grander quantity of fuel being introduced into the combustion chamber. Of the fuels tested, diesel had the highest CO emissions at 0.235%, while B20 in combination with 5% n-butanol and 75 ppm nanoparticles had the lowest emissions at 0.051%.

### UHC

Figure 10 shows the difference of UHC depending on the load. It was found that the UHC was minimized with ternary fuel blends of B20 and alcohol additives. The reduction in UHC with the addition of alcohol is mainly attributed to the increased combustion efficiency, the improved air–fuel mixture, the oxygen content in the alcohol molecules and the ability to work with leaner air–fuel mixtures. These elements lead to additional whole oxidation of the fuel, resulting in a decrease in UHC (El-Sheekh et al., 2022; Mobasheri et al., 2023; Preuß et al., 2018; Saravanan et al., 2020a, 2020b; Zhao et al., 2022). Furthermore, the admixture of

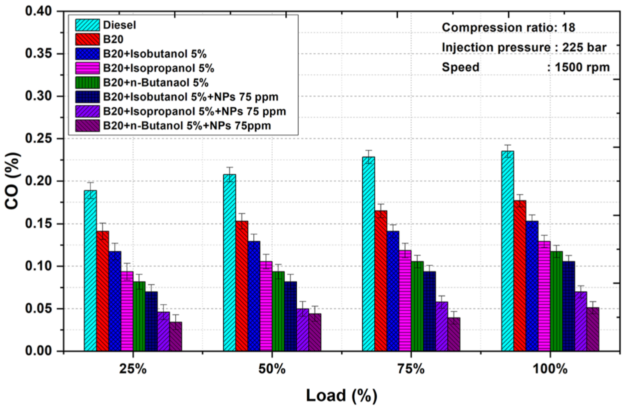

**Fig. 9** CO versus load

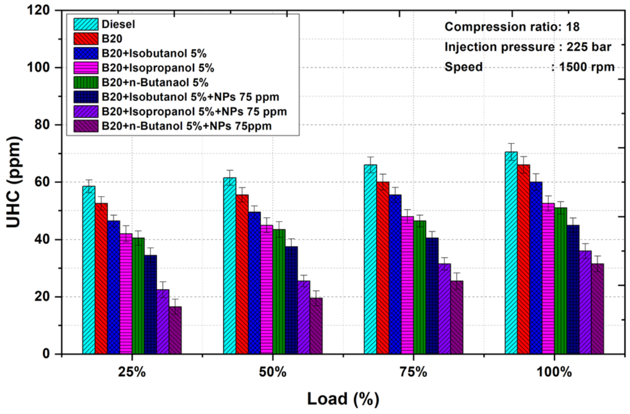

**Fig. 10** UHC versus load

$TiO_2$ nanoparticles in the ternary fuel mixture serves as a catalyst and favours the propagation of the flame. The elevated oxygen share of alcohol is marked by little unburned hydrocarbons during combustion (Illipilla et al., 2023; Jaikumar et al., 2021; Kunchi et al., 2024). Finally, the UHC showed an upward trend at higher loads. Increasing the load increases the combustion temperature, which leads to improved combustion efficiency and thus increases the UHC. The B20 blend with 5% n-butanol and 75 ppm nanoparticles had the lowest UHC emissions at 31 ppm, while diesel had the highest UHC emissions of the fuels tested at 70 ppm.

### $NO_x$

Figure 11 shows the change in $NO_x$ against load. The $NO_x$ values of the ternary fuel based on B20 and isobutanol, isopropanol, and n-butanol are significantly higher than for diesel as a result of the surge in the overall combustion temperature. The temperature exerts a significant impact on the production of $NO_x$, facilitating its release more readily at elevated combustion temperatures (El-Sheekh et al., 2022; Mobasheri et al., 2023; Mujtaba et al., 2020; Zhao et al., 2022). However, the distribution of $TiO_2$ nanoparticles in the alcohol mixture directed to a noteworthy drop in $NO_x$ than diesel, as the average combustion temperature was lowered due to the amended convective heat transfer. In addition, there was a reduction in $NO_x$, perhaps owing to improved catalytic activity and the effective removal of nitrogen oxides by the nanoparticles (Jaikumar et al., 2021; Reddy et al., 2023; El-Seesy et al., 2019; Kunchi et al., 2024). Finally, the higher loads lead to an increase in $NO_x$ emissions due to the higher combustion temperatures. The combination of B20, 5% n-butanol and 75 ppm nanoparticles had the lowest $NO_x$ emissions of the fuels tested at 1245 ppm. In contrast, B20 in combination with 5% n-butanol had the highest $NO_x$ emissions at 1538 ppm.

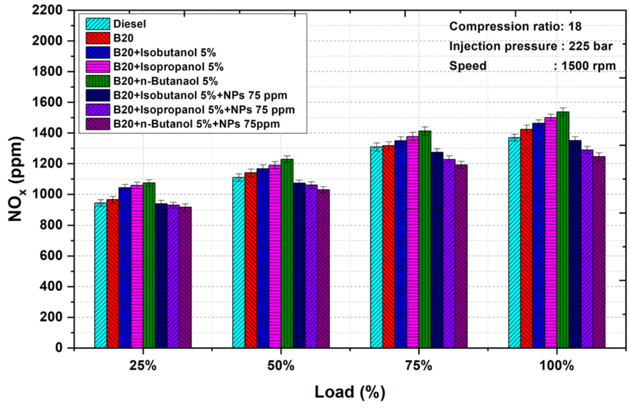

**Fig. 11** $NO_x$ versus load

### Smoke opacity

Figure 12 demonstrates the smoke development as a function of the load for various ternary fuel mixtures with dispersed nanoparticles. The highest smoke generation is observed for diesel compared to alcohol-added B20 and alcohol blends dispersed with $TiO_2$ nanoparticles. In addition, lower smoke production was observed with alcohol additives in B20, which is due to the presence of excess oxygen that minimizes the production of soot, an important component of smoke (Sayyed et al., 2023; Zuo et al., 2022; El-Sheekh et al., 2022). In addition, the improved atomization of the fuel into tiny droplets and a more uniform mixture leads to lower smoke emissions. Besides, an extra decrease in smoke emission was observed when the $TiO_2$ nanoparticles are dispersed in alcohol fuel mixtures due to catalytic capabilities (Jaikumar et al., 2021; Kunchi et al., 2024; Reddy et al., 2023). The higher combustion temperatures led to an increase in smoke development with increasing load. At full load, diesel had the highest smoke emissions at 43.15%, while B20 in combination with 5% n-butanol and 75 ppm nanoparticles had the lowest smoke emissions of the fuels tested at 32.63%.

## Conclusions

On the basis of the investigation carried out, the ensuing conclusions were taken:

- The physicochemical properties of hybrid biodiesel were within the limits of the ASTM guidelines. The hybrid biodiesel has a higher cetane value than conventional diesel fuel.
- The stability was higher for n-butanol based ternary nanofuel than for the other ternary nanofuels.

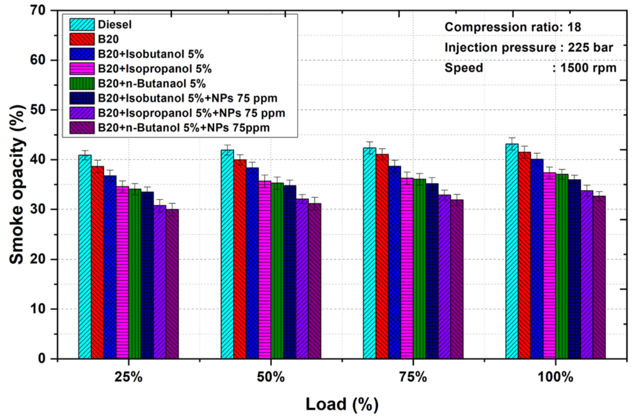

**Fig. 12** Smoke opacity versus load

- The $TiO_2$ nanoparticles dispersed the ternary fuel combination disclosed improved BTE and reduced BSFC compared to the individual alcohol blends. The nanoparticles containing n-butanol showed better performance compared to the other samples. The improved BTE of 26.91% and reduced BSFC of 0.173 kg/kWh were observed for the fuel sample.
- The similar fuel combination has also shown improvements in CP and NHRR associated to diesel and the values are 68.12 bar and 70.14 J/°CA for the n-butanol based ternary nanofuel.
- Lastly, n-butanol based ternary nanofuel showed the most favourable results and resulted in the lowest emissions of CO, UHC, $NO_x$, and smoke, which were 0.051%, 31 ppm, 1245 ppm, and 32.63%, respectively.

The results indicate that the incorporation of $TiO_2$ nanoparticles into ternary fuel blends can facilitate their use in a diesel engine without the need for modifications.

**Acknowledgements** The authors would like to thank the Department of Mechanical Engineering, GITAM (Deemed to be University), Visakhapatnam, HPCL Visakhapatnam, and Lords Institute of Engineering and Technology, Hyderabad, for their valuable support in the successful conduct of the experiments.

**Funding** Not applicable.

## Declarations

**Conflict of interest** No.

**Ethical Approval** Not applicable.

## References

Anantha, P. H. S., & Mohanty, D. K. (2024). Enhancement of combustion, performance and emission characteristics of diesel engines fuelled with jatropha-karanja biodiesel using EGM and TGME as additive. *Energy*, 131523.

Chaurasiya, P. K., Singh, S. K., Dwivedi, R., & Choudri, R. V. (2019). Combustion and emission characteristics of diesel fuel blended with raw jatropha, soybean and waste cooking oils. *Heliyon, 5*(5).

El-Seesy, A. I., & Hassan, H. (2019). Investigation of the effect of adding graphene oxide, graphene nanoplatelet, and multiwalled carbon nanotube additives with n-butanol-Jatropha methyl ester on a diesel engine performance. *Renewable Energy, 132*, 558–574.

El-Seesy, A. I., Nour, M., Attia, A. M., He, Z., & Hassan, H. (2020). Investigation the effect of adding graphene oxide into diesel/higher alcohols blends on a diesel engine performance. *International Journal of Green Energy, 17*(3), 233–253.

El-Seesy, A. I., Nour, M., Hassan, H., Elfasakhany, A., He, Z., & Mujtaba, M. A. (2021). Diesel-oxygenated fuels ternary blends with nano additives in compression ignition engine: A step towards cleaner combustion and green environment. *Case Studies in Thermal Engineering, 25*, 100911.

El-Sheekh, M. M., Bedaiwy, M. Y., El-Nagar, A. A., ElKelawy, M., & Bastawissi, H. A. E. (2022). Ethanol biofuel production and characteristics optimization from wheat straw hydrolysate: Performance and emission study of DI-diesel engine fueled with diesel/biodiesel/ethanol blends. *Renewable Energy, 191*, 591–607.

Garugubilli, R., Prasad, V. V. S., & Sagari, J. (2024). Experimental investigation on diesel engine operating with CuO nanoparticles dispersed *Azadirachta indica* biodiesel. *International Journal of Thermofluids*, 100641.

Illipilla, M., Lankapalli, S. V. P., & Sagari, J. (2023). Experimental study on a diesel engine fueled with *Semecarpus anacardium* biodiesel containing dispersed $TiO_2$ nanoparticles: Performance, combustion, and emission analyses. *Energy, Ecology and Environment, 8*(2), 113–128.

Jaikumar, S., Srinivas, V., & Rajasekhar, M. (2021). Influence of dispersant added nanoparticle additives with diesel-biodiesel blend on direct injection compression ignition engine: Combustion, engine performance, and exhaust emissions approach. *Energy, 224*, 120197.

Kari, J., Vanthala, V. S. P., & Sagari, J. (2024). Performance and emission characteristics of a diesel engine fuelled with Mesua ferrea biodiesel with chromium oxide ($Cr_2O_3$) nanoparticles: Experimental approach and response surface methodology. *International Journal of Thermofluids*, 100637.

Killol, A., Reddy, N., Paruvada, S., & Murugan, S. (2019). Experimental studies of a diesel engine run on biodiesel n-butanol blends. *Renewable Energy, 135*, 687–700.

Kunchi, L. R., Bhatti, S. K., Lankapalli, S. V. P., & Sagari, J. (2024). Effect of multi ferrites nanoparticles added *Terminalia bellirica* biodiesel on diesel engine: Combustion, performance, and emission studies. *International Journal of Thermofluids, 22*, 100652.

Liang, J., Zhang, Q., Chen, Z., & Zheng, Z. (2021). The effects of EGR rates and ternary blends of biodiesel/n-pentanol/diesel on the combustion and emission characteristics of a CRDI diesel engine. *Fuel, 286*, 119297.

Mahlia, T. M. I., Syazmi, Z. A. H. S., Mofijur, M., Abas, A. P., Bilad, M. R., Ong, H. C., & Silitonga, A. S. (2020). Patent landscape review on biodiesel production: Technology updates. *Renewable and Sustainable Energy Reviews, 118*, 109526.

Mobasheri, R., Aitouche, A., Pourtaghi Yousefdeh, S., & Zarenezhad Ashkezari, A. (2023). Assessing the impact of ethanol/biodiesel/diesel blends and nanoparticle fuel additives on performance and emissions in a DI diesel engine with EGR integration: An experimental study. *Processes, 11*(4), 1266.

Mujtaba, M. A., Kalam, M. A., Masjuki, H. H., Gul, M., Soudagar, M. E. M., Ong, H. C., & Yusoff, M. (2020). Comparative study of nanoparticles and alcoholic fuel additives-biodiesel-diesel blend for performance and emission improvements. *Fuel, 279*, 118434.

Nutakki, P. K., Gugulothu, S. K., Ramachander, J., & Sivasurya, M. (2022). Effect Of n-amyl alcohol/biodiesel blended nano additives on the performance, combustion and emission characteristics of CRDi diesel engine. *Environmental Science and Pollution Research*, 1–16.

Parida, M. K., Mohapatra, P., Patro, S. S., & Dash, S. (2024). Effect of $TiO_2$ nano-additive on performance and emission characteristics of direct injection compression ignition engine fueled with Karanja biodiesel blend. *Energy Sources, Part a: Recovery, Utilization, and Environmental Effects, 46*(1), 7521–7530.

Preuß, J., Munch, K., & Denbratt, I. (2018). Performance and emissions of long-chain alcohols as drop-in fuels for heavy duty compression ignition engines. *Fuel, 216*, 890–897.

Potnuru, B. D., Indra Kiran, N. V. N., & Sagari, J. (2025). Predicting the operating characteristics of a diesel engine running on a ternary fuel blend of alcohol, hybrid biodiesel and diesel with nanoparticles: Experimental analysis and response surface methodology. *International Journal of Thermofluids, 26*, 101063.

Rangabashiam, D., Munuswamy, D. B., Duraiswamy Balasubramanian, S., & Christopher, D. (2024). Performance, emission, and combustion analysis on diesel engine fueled with blends of neem biodiesel/diesel/additives. *Energy Sources, Part a: Recovery, Utilization, and Environmental Effects, 46*(1), 8059–8069.

Reddy, V. L., Sagari, J., Vadapalli, S., & Prasad, V. V. S. (2023). Investigation of operating parameters of diesel engine fueled with $SiO_2$ nanoparticles and *Abrus precatorius* biodiesel: Experimental approach and response surface methodology. *Water, Air, & Soil Pollution, 234*(7), 416.

Saravanan, A., Murugan, M., Reddy, M. S., & Parida, S. (2020a). Performance and emission characteristics of variable compression ratio CI engine fueled with dual biodiesel blends of Rapeseed and Mahua. *Fuel, 263*, 116751.

Saravanan, S., Kaliyanasunder, R., Kumar, B. R., & Rao, G. L. N. (2020b). Effect of design parameters on performance and emissions of a CI engine operated with diesel-biodiesel-higher alcohol blends. *Renewable Energy, 148*, 425–436.

Saxena, V., Kumar, N., & Saxena, V. K. (2019). Multi-objective optimization of modified nanofluid fuel blends at different $TiO_2$ nanoparticle concentration in diesel engine: Experimental assessment and modeling. *Applied Energy, 248*, 330–353.

Sayyed, S., Das, R. K., Kulkarni, K., Alam, T., & Eldin, S. M. (2023). Influence of additive mixed ethanol-biodiesel blends on diesel engine characteristics. *Alexandria Engineering Journal, 71*, 619–629.

SenthilKumar, S., & Rajan, K. (2022). Performance and emission characteristics of diesel engine using biodiesel with the effect of dimethyl carbonate (DMC) fumigation. *Energy Sources, Part a: Recovery, Utilization, and Environmental Effects, 44*(2), 2986–2998.

Srikanth, H. V., Sharanappa, G., Manne, B., & Kumar, S. B. (2021). Niger seed oil biodiesel as an emulsifier in diesel-ethanol blends for compression ignition engine. *Renewable Energy, 163*, 1467–1478.

Zhao, W., Yan, J., Gao, S., Lee, T. H., & Li, X. (2022). The combustion and emission characteristics of a common-rail diesel engine fueled with diesel, propanol, and pentanol blends under low intake pressures. *Fuel, 307*, 121692.

Zuo, L., Wang, J., Mei, D., Dai, S., & Adu-Mensah, D. (2022). Experimental investigation on combustion and (regulated and unregulated) emissions performance of a common-rail diesel engine using partially hydrogenated biodiesel-ethanol-diesel ternary blend. *Renewable Energy, 185*, 1272–1283.